

# Structural integration of strain gages

Prof. Dr.-Ing. Alexander Horoschenkoff  
Dipl.-Ing. Sebastian Klein  
Dr.-Ing. Karl-Heinz Haase

### **Important notice**

We know from experience that the processes, measurement tools, methods and materials mentioned or recommended in this brochure are reliable and suitable for the purpose described and also conform to the state of the art. They are to be meant as guidance and advice for the strain gage user. However, as applications are so diverse and conditions so complex, it is not possible for either Hottinger Baldwin Messtechnik GmbH or the authors to offer any guarantees, nor can they be held liable in any way whatsoever for any claims derived therefrom. So for critical situations, it is advisable to first make a preliminary test, taking all the specific conditions into account. The user is responsible for complying with all relevant safety rules and working regulations.

Neither the publisher nor the authors are aware of any industrial property rights that would be affected by these implementations, although this certainly cannot be excluded.

#### **Note:**

The numbers in square brackets (e.g. [1]) relate to the reference documentation.

2006

Printed in Germany

All rights reserved. No part of this document may be reproduced in whole or in part in any form or by any means, or translated, without the express written permission of the authors or publishers. Extracts may be photocopied for personal use.

# Structural integration of strain gages

Prof. Dr.-Ing. Alexander Horoschenkoff  
Dipl.-Ing. Sebastian Klein  
Dr.-Ing. Karl-Heinz Haase

# Contents

<b>Introduction</b> .....	<b>6</b>
<b>1 Fiber composites</b> .....	<b>8</b>
1.1 Fiber types .....	8
1.2 Theoretical principles .....	9
1.3 Production processes .....	11
<b>2 Fiber composite theory</b> .....	<b>14</b>
2.1 Orthotropic material response .....	14
2.2 Material matrix of the unidirectionally oriented single layer .....	14
2.3 Multilayer composites .....	15
2.4 Thermoelastic response .....	17
2.5 Stiffness of the unidirectionally reinforced single layer .....	17
<b>3 Calculating the stiffness matrix of a multilayer composite in the global coordinate system from the properties of single layers</b> .....	<b>19</b>
3.1 Transformation matrices $[T_1]$ and $[T_2]$ : .....	19
3.2 Transformation of the stiffness matrix for the single layer: .....	19
3.2.1 Transformation for the $0^\circ$ layer .....	20
3.2.2 Transformation for the $90^\circ$ layer .....	20
3.2.3 Transformation for the $+45^\circ$ layer .....	20
3.2.4 Transformation of thermal expansion coefficients .....	22
3.3 Calculating the stiffness matrix for the multilayer composite in the global system from the sum of the single layers .....	22
3.4 Calculating the deformations of the entire composite .....	24
3.5 Transformation of $[\varepsilon]_{xy}$ to the local system of single layer $k$ .....	25
3.6 Calculating the intralaminar stresses in single layer $k$ .....	25
3.7 Calculating the expansion coefficients of the multilayer composite .....	25
3.8 Determining the intralaminar shear properties ( $G_{12}$ and $\tau_{12\max}$ ) on the tensile test specimen with fiber orientation $\pm 45^\circ$ .....	25
<b>4 Interlaminar stresses and rate of energy release in the multilayer composite</b> .....	<b>27</b>
<b>5 Integrating strain gages</b> .....	<b>28</b>
5.1 Structural mechanical aspects .....	28
5.1.1 The effect of integration on the interlaminar properties of the composite .....	28
5.1.2 The effect of the orientation of adjacent layers on measurement accuracy .....	30
5.1.3 Depth of strain gage integration for reducing the level of strain .....	30
5.1.4 Dependency of measurement error on strain gage orientation .....	32
5.1.5 The effect of heat generation for integrated strain gages .....	38
5.1.6 Temperature compensation for fiber composites .....	38
5.1.7 Effect of transverse sensitivity .....	39
5.1.8 Effect of strain gage sensitivity perpendicular to the measuring grid plane .....	42

5.2	Description of the strain gage.....	42
5.2.1	Structure and attachment of the strain gage.....	43
5.2.2	Function of strain gage contact pins.....	44
5.2.3	Technical properties of the strain gage.....	45
5.3	Strain gage integration.....	46
5.3.1	Strain gage positioning.....	46
5.3.2	Strain gage fixing.....	47
5.3.3	Laminating and applying more layers.....	48
5.3.4	Shortening and covering the pins.....	50
5.3.5	Hints on removal from the mold.....	51
5.4	Connecting the measuring leads.....	52
5.4.1	Removing the insulation.....	52
5.4.2	Contacting the pins.....	53
<b>6</b>	<b>Measuring point protection.....</b>	<b>54</b>
<b>7</b>	<b>Bibliography.....</b>	<b>55</b>

# Introduction

Fiber composites have arrived in many areas of our modern industrial society and because of their special properties, are continually gaining importance. Today's innovative applications are not just found in aerospace or motor racing, but also in power engineering and medical technology, in civil engineering and in sports and leisure equipment. As our knowledge of the advantages of fiber composites and their properties increases and not least as the prices for aluminum and steel continue to rise, there is a substantial increase in the number of applications of these materials.

Accurate knowledge of the loading situation is just as significant for fiber composites as it is, in the sense of endurance strength, for conventional materials. Structural measurement technology for the systematic optimization of fiber composite components is a typical representative here. It is also becoming more and more important, with regard to the manufacturer's warranty responsibility, to have sensor technology specifically adapted to the properties of this material to be used for load analysis and component monitoring during operation.

The methods of analysis applied to metallic materials are either not at all appropriate for fiber composites, or can only be used in certain situations.

This brochure should provide both theoretical and practical hints about how to evaluate the mechanical performance of fiber composites experimentally.

Investigations of this type are new and we have to assume that there will be a vast increase in the number of publications dealing with experimental testing and evaluation of the mechanical influences and stresses. This article neither can nor should lay claim to be exhaustive.

Stress analysis with strain gages (SGs) is a commonly used method of experimentally determining the material stresses of all materials relevant to production engineering. Historically, this typically focused predominantly on metallic materials.

Fiber composites have different basic properties, which differ considerably from metals. Extreme strain of up to  $\pm 20,000 \mu\text{m/m}$  ( $\pm 2\%$ ) on the edge fibers and their anisotropic material response are characteristic indications. The extreme strain capacity is a particular problem for metallic strain gage measuring grids, because of the typical resistance to alternating loads found here. In strain gage force transducer construction, for example, the metallic transducer elements, the resistance loops of the grid, are deflected by  $\pm 1,000 \mu\text{m/m}$  ( $\pm 0.1\%$ ). More extreme mechanical stresses can cause the strain gage to fail prematurely.

The special construction of fiber composite components, where individual layers are stacked one on top of the other, allows strain gages to be embedded during production. The motivation for integration often differs and is specific to the particular application. For example, integration is to be recommended if the bending strain is extreme, as the integration depth can be used to adapt the level of strain to the strain level of the strain

gage. As you get closer to the component zone where bending is neutral, the mechanical stress transferred to the electrical measuring grid of the strain gage is also reduced.

Strain gages can also be installed during production to places that are later no longer accessible. This extends the range of measurement positions and allows measurements to be taken on complex structural designs with hollow spaces, or between adhesive joints.

In addition to this, fiber composites that as a result of structural integration have integrated strain sensors can provide, a priori, a greater degree of protection for the measuring point, which often cannot be ensured by conventional strain gage protective measures, such as covering agents.

This embedded installation of the strain gage is also an advantage for fluidic components or components that are aerodynamically sensitive.

In collaboration with the Department of Mechanical, Automotive and Aeronautical Engineering at the University of Applied Sciences in Munich, investigations are being carried out under the leadership of Prof. Dr A. Horoschenkoff on strength behavior and questions of the physical elasticity of structurally integrated applications. This HBM application document is concerned with bringing home to our readers the relevant questions in connection with fiber composite technology and keeping them informed about the knowledge we have gained and the investigations we have carried out. We have consulted with users of strain gage technology who already have some experience in this field. The basics of strain gage measurement technology (working principles, wiring types, etc.), are largely given. A great deal of supplementary literature is available (such as K. Hoffmann "An Introduction to Measurements using Strain Gages", [7]).

# 1 Fiber composites

As is made clear by the term “fiber composite“, these materials are a composite of reinforcing fibers with a plastic matrix to bind the fibers. A brief summary of fiber types and processing methods should make it easier to understand the subsequent chapters.

## 1.1 Fiber types

Plastics technology uses different fiber types to reinforce the composite:

- Glass fiber (GFRP)

Glass fibers are in widespread use as a reinforcement material for fiber composites and they have excellent mechanical, thermal, dielectric and chemical properties. Glass fibers are non-combustible, thermally stable to about 400°C and resistant to most chemicals and weather conditions. The strength behavior of the fibers is better than that of many metallic materials. Compared to that of metal, the stiffness (modulus of elasticity) of glass fiber laminates is relatively low, so with a stiffness-specific component design, the wall thickness required cancels out the weight advantage. Composites made of glass fibers are called GFRP (glass fiber reinforced plastic).

- Carbon fibers (CFRP)

The vast field of application for carbon fibers (C-fibers) nowadays is not just down to their outstanding properties. Constantly improving prices and the demand for ever lighter structures are further factors in this popularity. So the expensive “high-tech fibers” that were once used for aerospace applications are now also found in production vehicles and in the sports goods industry.

Good strength and a high modulus of elasticity, low density and fatigue, low thermal conductivity and temperature dilatation but also electric conductivity and chemical resistance are the distinguishing features of carbon fibers. C-fibers can be over 95% pure carbon.

- Synthetic fibers (SFRP)

By synthetic fibers, we mean fibers made of synthetic (not natural), organic polymers, that is, of more or less long-chain molecules. Important representatives of these fibers are polyamide fibers (nylon), polyester fibers, fibers made of polypropylene and aramid fibers. Because of the high crystalline content and the orientation of the molecule chains, the distinguishing features of synthetic fibers are extremely good strength and breaking strain, high tenacity and a good energy absorption capacity and low fatigue.



But because of the polymer molecular structure, they have ageing characteristics and tend to absorb moisture and creep.

- Natural fibers

These differ not only in their mechanical and chemical properties, but also in their production and their fields of application.

Natural fiber representatives include flax, sisal and coconut fibers, as well as spun silk, cotton and jute. They are distinguished by their natural material cycle – regenerative raw material and CO<sub>2</sub> recycling during energy recovery - and by their good price. The disadvantages of natural fibers are the high specific modulus of elasticity at low strength, high moisture absorption (a tendency to swell) and vast fluctuations in the quality of the raw material.

		<b>Carbon fibers HT</b>	<b>Glass fibers Low- alkali glass</b>	<b>Synthetic fibers Aramid LM</b>	<b>Natural fibers Flax</b>
<b>Strength <math>\sigma</math> [MPa]</b>		3,600	2,400	2,800	7,500
<b>Modulus of elasticity [MPa]</b>	E <sub>11</sub> E <sub>22</sub>	240,000 15,000	73,000 73,000	65,000 5,400	30,000 -
<b>Thermal expansion coefficient <math>\alpha</math> [<math>10^{-6}K^{-1}</math>]</b>	$\alpha_{11}$ $\alpha_{22}$	-1 10	5 5	-2 40	-
<b>Density <math>\rho</math> [g/cm<sup>3</sup>]</b>		1.78	2.6	1.44	1.48

Table 1.1: Characteristic values of the different fiber types

## 1.2 Theoretical principles

The mechanical properties are directly related to the length of the reinforcing fibers. They are classified as short fibers, long fibers and directional continuous fibers (Table 1.2-1).


The fibers are not normally aligned when plastics are reinforced with short and long fibers. Because the fibers are randomly arranged, the plastic is evenly reinforced in all directions, so that the isotropic material properties can be assumed.

In contrast to this, when reinforcement is provided by directional continuous fibers, the reinforcement of the plastic is always assumed to be directionally dependent. Plastics with directional continuous fibers have anisotropic material properties. The directional dependency of the fiber arrangement and the alignment of the strain gage measuring grid must be taken into account when measuring strain on fiber composite structures.

As well as the length of the fibers, the fiber material is also crucially important for the reinforcing effect. Glass fibers and carbon fibers are used most frequently.

Because of the high specific modulus of elasticity, carbon fibers are suitable for making components that require a high level of stiffness and strength.

On the other hand, glass fibers have a low modulus of elasticity with good strength. This makes them suitable for reinforcing components requiring a high level of elasticity (see Table 1.2-1).



Properties	Pure resin	Glass-fiber reinforcement		
		Short fibers	Long fibers	Directional continuous fibers
Fiber length [mm]	0	up to 5	100	continuous
Fiber volume [Vol.%]	0	30	40	60
Density [g/cm <sup>3</sup> ]	1.2	1.5	1.7	2.1
Mod. of elasticity [MPa]	3,000	6,000	13,000	20,000 - 40,000
Strength [MPa]	70	100	210	600 - 2,000
Material response		isotropic		anisotropic

Table 1.2-1: The effect of the fiber length of glass fibers on mechanical properties for the reinforcement of plastics [4]

As already mentioned, synthetic fibers and natural fibers are used as well as glass and carbon fibers.

## 1.3 Production processes

The processing of fiber-reinforced plastics is always dependent on the type of plastic, whether thermoplastic or duroplastic, and the length of the fibers.

Methods of processing fiber-reinforced thermoplastics:

- Injection molding (short fiber reinforced)
- Compression molding – glass mat reinforced thermoplastic (GMT)
- Injection before polymerization

Methods of processing fiber-reinforced duroplastics:

- R-RIM (Reinforced RIM)
- Prepreg processing and autoclave techniques
- Injection process (RTM and vacuum injection)
- Hand lay-up process
- Compression molding – SMC (Sheet Molding Compound)

The injection process, the hand lay-up process and prepreg processing in autoclaves are presented below, as these production techniques allow directional continuous fibers to be processed.

- Resin Transfer Molding (RTM):

With the RTM process, first the dry reinforcement material is placed in a double-shell mold or molding tool. Resin impregnation only takes place once the mold has been closed, when the (resin) matrix is injected or drawn into the mold. RTM (Resin Transfer Molding) is the name of the process by which the resin/hardener mix is taken under pressure from its original container into the mold. When making complicated components, it is useful to use preformed reinforcement materials. Thermoplastically bonded mats and fabrics, which have been preformed by heating beforehand, are mainly used. A second variant is the braided or wound "preforms", based on a mold core. Because of the low resin flow rate and the fixing of the fibers, the designated fiber orientation is retained.

Low viscosity epoxy and polyester resins are processed as the matrix. Suitable reinforcement is provided by glass, aramid and carbon fibers as woven and bonded

fabrics, webs, non-wovens and mats. Components up to about 3 m<sup>2</sup> in size can be made using this process. This is because limits are set by the necessity of using a double-shell molding tool, designed for an injection pressure of about 10 bar. The cycle time can be a few hours, depending on the resin.

- Prepreg processing in autoclaves:

The autoclave process is one of the most expensive and complicated processing methods. It is normally only applied when using prepregs. Prepregs are preimpregnated with a special resin and "gelated" reinforcing fibers, which are made by specialist companies as requested by the customer. Complicated components that can withstand high mechanical and thermal loads can be compression-molded from prepregs. The fiber volume content is about 60%, the entrained air content is extremely low. Because of high cost, the autoclave process is mainly used to make complex components with exacting requirements, such as in aerospace applications or in motor racing. To make prepreg laminates, the individual prepreg layers must be placed in the mold by hand or by a tapelayer and covered with perforated film, absorbent matting and a vacuum bag film. Before the construction is placed in the autoclaves, the vacuum is created and checked for leaks. At a pressure of up to 10 bar and a temperature of up to 200°C, the prepreg laminate takes several hours to harden and can be removed once it has cooled down and ventilated.

- Vacuum injection process:

Unlike the RTM and RIM processes the vacuum injection process works at a pressure of 1 bar. The essential difference is that with this method, a single-shell molding tool is used and with preforms with a mold core, the molding tool is dispensed with totally. This greatly reduces the high investment costs for the molding tool.

With the vacuum injection process, the fiber preform is placed in the mold and covered with a runner system for the resin and a vacuum bag film. Here the resin is drawn into the mold by the creation of the vacuum (approx. 1 bar) and is initially dispersed superficially on the runner system. It is only during the second stage that the resin is dispersed perpendicularly to the laminate plane and penetrates it in the thickness direction. Depending on the resin, curing takes place at temperatures between 20°C and 80°C.

This process is particularly suitable for components greater than 3 m<sup>2</sup> in size. Too much effort is required with the runner system to make this suitable for the relatively small tensile test specimens, despite the relatively low investment costs.

- Hand lay-up process

Hand lay-up is the oldest, simplest and most widespread process. The technical requirements are minimal, which is why it is mainly used for smaller batches (prototype construction), simpler component geometries and for mold construction. When mold resins are used, better surface qualities can be achieved. Curing virtually always takes place at normal pressure and room temperature. It is only necessary to increase the temperature for curing if the molds and the components are later to be exposed to greater thermal loading (> approx. 60°C).

With hand lay-up, a release agent is applied to the surface of the mold. Then the individual wet layers are placed into the mold one after the other. Brushes and grooved rollers are the main tools that are used to impregnate the layers with the resin. The final layer is often a peel ply. This ply fabric of nylon fibers can be "peeled off" after the resin has cured, which produces a definably rough and clean surface. For the most part, laminate curing takes place at normal pressure and room temperature. Curing only takes place in a vacuum at 1 bar negative pressure for optimized lightweight components. Certain resin systems, in particular resins for aircraft construction, need higher temperatures for optimum, full curing. The components are either conditioned additionally in the mold or after removal from the mold. The requisite temperatures for this are often 50 - 100 °C, depending on the resin system.

Liquid resins, in particular epoxy and polyester resins, are processed as the matrix. The reinforcement materials are often processed as rovings, woven and bonded fabrics and mats and consist of directional glass, aramid and carbon fibers.

## 2 Fiber composite theory

### 2.1 Orthotropic material response

Whereas with short and long fiber-reinforced plastics the material deformations can be calculated by the usual constitutive equations for isotropic materials, with fiber composites with directional continuous fibers, special constitutive equations for an orthotropic material response are applied because of the anisotropy.

With fiber composites reinforced with directional continuous fibers, the individual layers are placed one on top of the other in accordance with the desired reinforcing effect, thus constructing a laminate. The fiber reinforcement in the individual layer is often aligned in one direction (unidirectionally reinforced single layer or UD-single layer). Materials with these properties have orthotropic properties.

### 2.2 Material matrix of the unidirectionally oriented single layer

Because of the orthotropic response for the two-dimensional, even loading situation, the following characteristic values are required to describe the mechanical properties of fiber composites:

$E_{11}$ : modulus of elasticity along the fiber orientation

$E_{22}$ : modulus of elasticity across the fiber orientation

$\nu_{12}$ : Poisson's ratio (loading in direction 1, deformation in direction 2)

$\nu_{21}$ : Poisson's ratio (loading in direction 2, deformation in direction 1)

$G_{12}$ : shear modulus

Engineering constants on the unidirectionally reinforced single layers can be determined in tensile testing by relevant harmonization of the force and fiber directions. Direction 1 is identical here to the fiber direction and is designated as the  $0^\circ$  orientation.

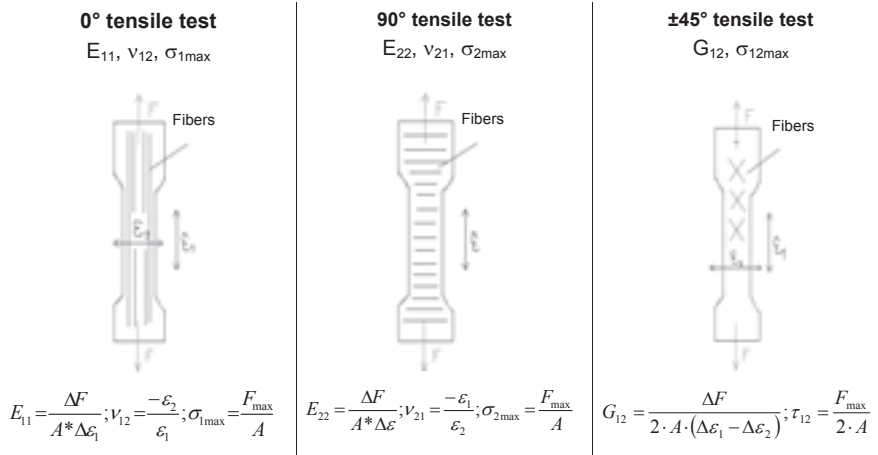


Fig. 2.2-1: Determining engineering constants for fiber composites EN 6031 and EN ISO 527-4

	GRP	CFP
$E_{11}$ [MPa]	40,000	160,000
$E_{22}$ [MPa]	9,000	9,500
$G_{12}$ [MPa]	3,500	5,500
$\nu_{12}$	0.21	0.28
$\alpha_1$	$6.24 \cdot 10^{-6}$ 1/K	$-4.35 \cdot 10^{-6}$ 1/K
$\alpha_2$	$0.35 \cdot 10^{-6}$ 1/K	$0.32 \cdot 10^{-6}$ 1/K

Table 2.2-1: Typical mechanical characteristic values of the individual layers of glass and carbon fiber reinforced plastics

## 2.3 Multilayer composites

A local 1-2 coordinate system and a global x-y coordinate system are introduced to describe the orientation of the individual layers in the composite. Direction 1 of the local coordinate system of the unidirectionally reinforced single layer is aligned along the fiber orientation. The fiber angle  $\theta$  describes the orientation of the single layer in the global system and is specified, by moving clockwise between direction 1 of the local system and direction x of the global system.

1-2: local coordinate system  
 x-y: global coordinate system

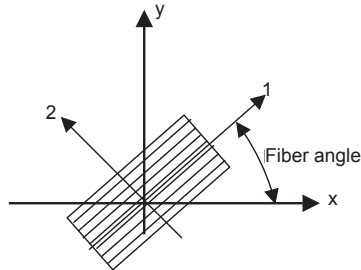


Fig. 2.3-1: Defining the fiber angle

There are various basic rules to follow in the arrangement of the layers in the composite. A symmetrical structure is crucially important here, that is, the layers must be arranged symmetrically to the center line of the composite, to stop the laminate warping under the thermal stresses applied during production.

Particularly significant here is a composite with a  $[+45^\circ, 0^\circ, -45^\circ, 90^\circ]_{\text{sym}}$  structure, which is also called a quasi-isotropic composite. This composite has material constants that are not dependent on the orientation. Table 2.2-1 shows typical mechanical properties for the unidirectionally reinforced single layer and the quasi-isotropic multilayer composite.

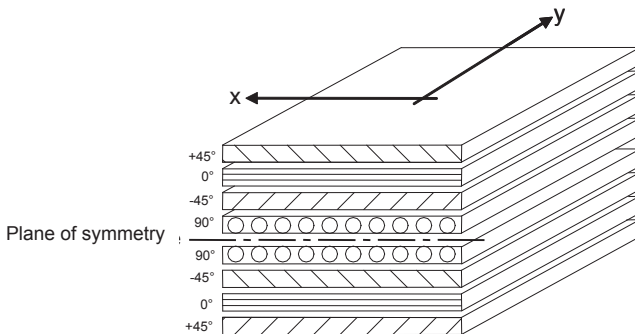


Fig. 2.3-2: Symmetrical structure of a quasi-isotropic laminate  $[+45^\circ, 0^\circ, -45^\circ, 90^\circ]_{\text{sym}}$



## 2.4 Thermoelastic response

The directionally dependent thermal expansion coefficients must be taken into account with regard to compensating for the thermal effects of strain measurements on fiber composites. Thus, for the unidirectionally reinforced single layer:

$$\begin{pmatrix} \varepsilon_1 \\ \varepsilon_2 \\ \gamma_{12} \end{pmatrix} = \begin{pmatrix} \alpha_1 \\ \alpha_2 \\ 0 \end{pmatrix} \Delta T$$

$\alpha_1$  = thermal expansion coefficient along the fiber orientation

$\alpha_2$  = thermal expansion coefficient across the fiber orientation

With carbon fiber reinforced plastics, the thermal expansion is usually relatively low (see Table 2.2-1).

## 2.5 Stiffness of the unidirectionally reinforced single layer

Conversion with compliance and stiffness is advisable to determine the properties of multilayer composites. The following correlation between the modulus of elasticity and compliance J applies:

$$J_{11} = \frac{1}{E_{11}}; \quad J_{22} = \frac{1}{E_{22}}; \quad J_{66} = \frac{1}{G_{12}}$$

By observing the energy, it is possible to demonstrate

$$J_{12} = J_{21} = \frac{-\nu_{12}}{E_{11}} = \frac{-\nu_{21}}{E_{22}};$$

This produces a compliance matrix [J] for orthotropic material.

$$[J] = \begin{bmatrix} J_{11} & J_{12} & 0 \\ J_{12} & J_{22} & 0 \\ 0 & 0 & J_{66} \end{bmatrix}$$

Thus, for stiffness matrix ( $C_{12} = C_{21}$ )

$$[C] = [J]^{-1} = \begin{bmatrix} C_{11} & C_{12} & 0 \\ C_{12} & C_{22} & 0 \\ 0 & 0 & C_{66} \end{bmatrix}$$

$$\begin{bmatrix} J_{11} & J_{12} & 0 \\ J_{12} & J_{22} & 0 \\ 0 & 0 & J_{66} \end{bmatrix} \begin{bmatrix} C_{11} & C_{12} & 0 \\ C_{12} & C_{22} & 0 \\ 0 & 0 & C_{66} \end{bmatrix} = \begin{bmatrix} 1 & 0 & 0 \\ 0 & 1 & 0 \\ 0 & 0 & 1 \end{bmatrix}$$

### 3 Calculating the stiffness matrix of a multilayer composite in the global coordinate system from the properties of single layers

If the properties of the unidirectionally reinforced single layer are known, it is possible to determine the properties of a composite that is built up of different, individual layers of any orientation.

#### 3.1 Transformation matrices $[T_1]$ and $[T_2]$ :

The prerequisite here is two transformation matrices  $T_1$  and  $T_2$ , which have to be defined for each individual layer in accordance with their fiber angle  $\theta$ :

$$[T_1] = \begin{bmatrix} m^2 & n^2 & 2mn \\ n^2 & m^2 & -2mn \\ -mn & mn & m^2 - n^2 \end{bmatrix} \quad [T_2] = \begin{bmatrix} m^2 & n^2 & mn \\ n^2 & m^2 & -mn \\ -2mn & 2mn & m^2 - n^2 \end{bmatrix}$$

Where:  $m = \cos \theta$ ;  $n = \sin \theta$

#### 3.2 Transformation of the stiffness matrix for the single layer:

In order to define the stiffness of the entire composite, the material matrix must be transposed into the global coordinate system for each individual layer of the entire composite.

$$\begin{bmatrix} \hat{C} \end{bmatrix} = [T_1]^{-1} * [C] * [T_2]$$

$[C]$  = stiffness matrix in the local 1-2 system

$\begin{bmatrix} \hat{C} \end{bmatrix}$  = stiffness matrix in the x-y global coordinate system

To calculate the properties of a quasi-isotropic laminate structure, the properties of the single layer have to be defined for the fiber angles  $0^\circ$ ,  $90^\circ$  and  $45^\circ$ .

### 3.2.1 Transformation for the 0° layer

Transformation for the 0° layer

$$\sin 0^\circ = 0 ; \cos 0^\circ = 1$$

$$[T_1] = \begin{bmatrix} 1 & 0 & 0 \\ 0 & 1 & 0 \\ 0 & 0 & 1 \end{bmatrix} \quad [T_2] = \begin{bmatrix} 1 & 0 & 0 \\ 0 & 1 & 0 \\ 0 & 0 & 1 \end{bmatrix}$$

$$\begin{bmatrix} \hat{C} \\ C \end{bmatrix} = \begin{bmatrix} 1 & 0 & 0 \\ 0 & 1 & 0 \\ 0 & 0 & 1 \end{bmatrix}^{-1} * \begin{bmatrix} C_{11} & C_{12} & 0 \\ C_{12} & C_{22} & 0 \\ 0 & 0 & C_{66} \end{bmatrix} * \begin{bmatrix} 1 & 0 & 0 \\ 0 & 1 & 0 \\ 0 & 0 & 1 \end{bmatrix} = \begin{bmatrix} C_{11} & C_{12} & 0 \\ C_{12} & C_{22} & 0 \\ 0 & 0 & C_{66} \end{bmatrix}$$

### 3.2.2 Transformation for the 90° layer

$$\sin 90^\circ = 1 ; \cos 90^\circ = 0$$

$$[T_1] = \begin{bmatrix} 0 & 1 & 0 \\ 1 & 0 & 0 \\ 0 & 0 & -1 \end{bmatrix} \quad [T_2] = \begin{bmatrix} 0 & 1 & 0 \\ 1 & 0 & 0 \\ 0 & 0 & -1 \end{bmatrix}$$

$$\begin{bmatrix} \hat{C} \\ C \end{bmatrix} = \begin{bmatrix} 0 & 1 & 0 \\ 1 & 0 & 0 \\ 0 & 0 & -1 \end{bmatrix}^{-1} * \begin{bmatrix} C_{11} & C_{12} & 0 \\ C_{12} & C_{22} & 0 \\ 0 & 0 & C_{66} \end{bmatrix} * \begin{bmatrix} 0 & 1 & 0 \\ 1 & 0 & 0 \\ 0 & 0 & -1 \end{bmatrix} = \begin{bmatrix} C_{22} & C_{12} & 0 \\ C_{12} & C_{11} & 0 \\ 0 & 0 & C_{66} \end{bmatrix}$$

### 3.2.3 Transformation for the +45° layer

$$\sin +45^\circ = \frac{1}{2}\sqrt{2} \quad ; \quad \cos +45^\circ = \frac{1}{2}\sqrt{2}$$

$$[T_1] = \begin{bmatrix} 0.5 & 0.5 & 1 \\ 0.5 & 0.5 & -1 \\ -0.5 & 0.5 & 0 \end{bmatrix} \quad [T_2] = \begin{bmatrix} 0.5 & 0.5 & 0.5 \\ 0.5 & 0.5 & -0.5 \\ -1 & 1 & 0 \end{bmatrix}$$

$$\begin{bmatrix} \hat{C} \\ C \end{bmatrix} = \begin{bmatrix} 0.5 & 0.5 & -1 \\ 0.5 & 0.5 & 1 \\ 0.5 & -0.5 & 0 \end{bmatrix}^{-1} * \begin{bmatrix} C_{11} & C_{12} & 0 \\ C_{12} & C_{22} & 0 \\ 0 & 0 & C_{66} \end{bmatrix} * \begin{bmatrix} 0.5 & 0.5 & 0.5 \\ 0.5 & 0.5 & -0.5 \\ -1 & 1 & 0 \end{bmatrix}$$

$$\left[ \hat{C} \right] = \begin{bmatrix} 0.25(C_{11} + C_{22}) + 0.5C_{12} + C_{66} & 0.25(C_{11} + C_{22}) + 0.5C_{12} - C_{66} & 0.25(C_{11} - C_{12}) \\ 0.25(C_{11} + C_{22}) + 0.5C_{12} - C_{66} & 0.25(C_{11} + C_{22}) + 0.5C_{12} + C_{66} & 0.25(C_{11} - C_{12}) \\ 0.25(C_{11} - C_{22}) & 0.25(C_{11} - C_{12}) & 0.25(C_{11} + C_{22}) - 0.5C_{12} \end{bmatrix}$$

Thus, for the transformation of the engineering constants:

$$\frac{1}{E_x} = \frac{1}{E_{11}} \cos^4 \varphi + \left( \frac{1}{G_{12}} - \frac{2\nu_{12}}{E_{11}} \right) \sin^2 \varphi \cos^2 \varphi + \frac{1}{E_{22}} \sin^4 \varphi$$

$$\nu_{xy} = E_x \left[ \frac{\nu_{12}}{E_{11}} (\sin^4 \varphi + \cos^4 \varphi) - \left( \frac{1}{E_{11}} + \frac{1}{E_{22}} - \frac{1}{G_{12}} \right) \sin^2 \varphi \cos^2 \varphi \right]$$

$$\frac{1}{E_y} = \frac{1}{E_{11}} \sin^4 \varphi + \left( \frac{1}{G_{12}} - \frac{2\nu_{12}}{E_{11}} \right) \sin^2 \varphi \cos^2 \varphi + \frac{1}{E_{22}} \cos^4 \varphi$$

$$\frac{1}{G_{xy}} = 2 \left( \frac{2}{E_{11}} + \frac{2}{E_{22}} + \frac{4\nu_{12}}{E_{11}} - \frac{1}{G_{12}} \right) \sin^2 \varphi \cos^2 \varphi + \frac{1}{G_{12}} (\sin^4 \varphi + \cos^4 \varphi)$$

Figs. 3.2.3-1 and 3.2.3-2 clearly show the directional dependency of the laminate values for the various structures.

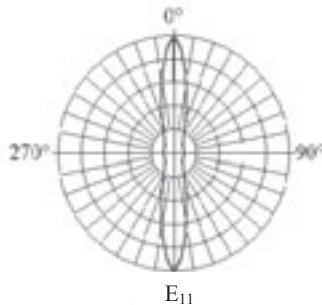


Fig. 3.2.3-1: Dependency of the modulus of elasticity on the fiber angle for the unidirectionally reinforced single layer

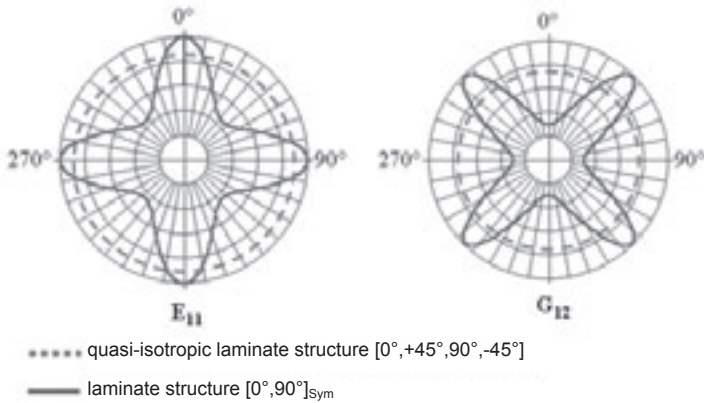


Fig. 3.2.3-2: Dependency of  $E_{11}$  and  $G_{12}$  on the fiber angle for two different laminate structures

### 3.2.4 Transformation of thermal expansion coefficients

The following applies to the transformation of thermal expansion coefficients between local and global properties:

$$(\alpha)_{12} = [T_2] \cdot (\alpha)_{xy} \quad \text{and} \quad (\alpha)_{xy} = [T_2]^{-1} \cdot (\alpha)_{12}$$

This allows the thermal expansion response to be defined for each  $\theta$  fiber angle.

## 3.3 Calculating the stiffness matrix for the multilayer composite in the global system from the sum of the single layers

The stiffness matrix of the entire composite can be defined from the properties of the single layers when the single layer is transposed into the global system in accordance with its orientation. Thus:

$$[A] = \sum_{k=1}^n [\hat{C}] \cdot h_k$$

$[A]$  = stiffness matrix of the composite in the x-y global system

$[\hat{C}]$  = stiffness matrix of single layer k in the x-y global system

n = number of layers

$k$  = continuous index ( $k = 1$  to  $n$ )

$h_k$  = thickness of single layer  $k$

The following matrix is produced for laminates with a symmetrical structure:

$$[A] = \begin{bmatrix} A_{11} & A_{12} & 0 \\ A_{12} & A_{22} & 0 \\ 0 & 0 & A_{66} \end{bmatrix}$$

The Kirchhoff hypothesis for plates and shells is a prerequisite. There must be strain compatibility for this 2-dimensional situation with stresses in the laminate plane (shell theory). This means that when there is tensile or compressive loading in the laminate plane, all the individual layers of the composite undergo even deformation, whatever their orientation. In contrast, the stresses vary in the individual layers (intralaminar stresses). The level of the stresses in the single layers is dependent on the stiffness of the single layer to the force direction. Layers with good stiffness in the force direction (fiber orientation and force direction coincide) have a high level of intralaminar stress. Layers with little stiffness to the force direction (the angle of the fibers to the force direction differs from 0 degrees) have low intralaminar stress.

When there is bending moment loading, a linear strain progression also develops, with areas under tensile and compressive loading and a neutral axis. Figs. 3.3-1 and 3.3-2 show typical strain and stress distribution for the quasi-isotropic composite during unidimensional loading.

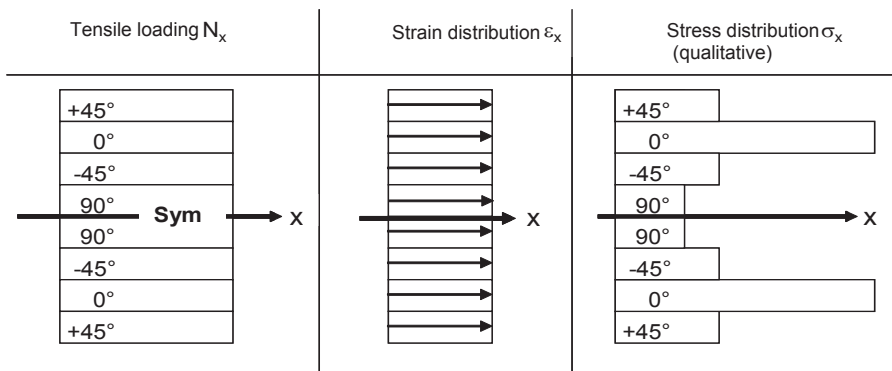


Fig. 3.3-1: Strains and stresses in the quasi-isotropic composite during tensile loading

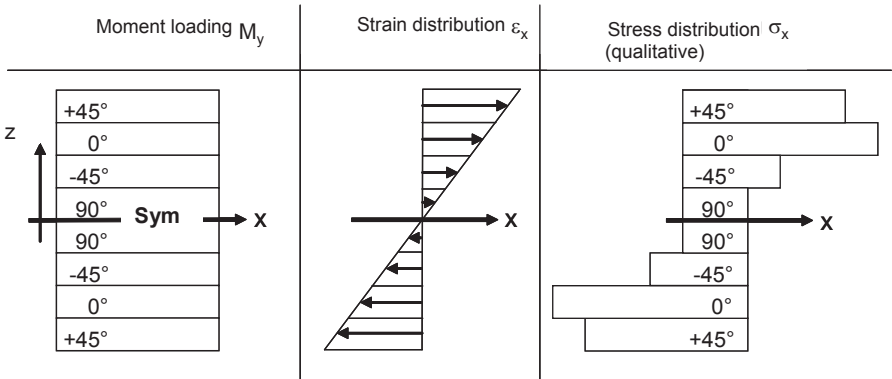


Fig. 3.3-2: Strains and stresses in the quasi-isotropic composite during moment loading

### 3.4 Calculating the deformations of the entire composite

If the stiffness matrix of the entire composite is known, the deformations of the entire composite can be calculated. Thus, for an even load situation:

$$[\varepsilon]_{xy} = \begin{bmatrix} \varepsilon_x \\ \varepsilon_y \\ \gamma_{xy} \end{bmatrix} = \begin{bmatrix} A_{11} & A_{12} & A_{16} \\ A_{21} & A_{22} & A_{26} \\ A_{61} & A_{62} & A_{66} \end{bmatrix}^{-1} \begin{bmatrix} N_x \\ N_y \\ N_{xy} \end{bmatrix}$$

$[\varepsilon]_{xy}$  = laminate strain in the x-y global system

$$[N]_{xy} = \begin{bmatrix} N_x \\ N_y \\ N_{xy} \end{bmatrix} \quad \text{Stress vector of the composite in the global x-y coordinate system}$$



### 3.5 Transformation of $[\varepsilon]_{xy}$ to the local system of single layer k

To make it possible to calculate the stresses in the single layer, the global deformations must be transformed to the local system of each individual layer.

$$[\varepsilon]_{12}^k = [T_2]^k [\varepsilon]_{xy}$$

### 3.6 Calculating the intralaminar stresses in single layer k

Now the local stresses of each individual layer can be calculated.

$$\begin{bmatrix} \sigma_1 \\ \sigma_2 \\ \tau_{12} \end{bmatrix}^k = \begin{bmatrix} C_{11} & C_{12} & C_{16} \\ C_{12} & C_{22} & C_{26} \\ C_{61} & C_{62} & C_{66} \end{bmatrix}^k \begin{bmatrix} \varepsilon_1 \\ \varepsilon_2 \\ \gamma_{12} \end{bmatrix}^k$$

### 3.7 Calculating the expansion coefficients of the multilayer composite

It is possible to define the thermal expansion response of the multilayer composite from the thermal expansion coefficients of the unidirectionally reinforced single layer.

$$[\alpha] = \frac{1}{[A]} \sum [C]^k \{\alpha\}_{xy}^k h^k$$

### 3.8 Determining the intralaminar shear properties ( $G_{12}$ and $\tau_{12\max}$ ) on the tensile test specimen with fiber orientation $\pm 45^\circ$

Now it is possible to demonstrate that with the  $\pm 45^\circ$  laminate structure, the intralaminar shear properties of the individual layer can be defined.

$$[\sigma]_{12} = [T_1][\sigma]_{xy}$$

for +45°:

$$\begin{bmatrix} \sigma_1 \\ \sigma_2 \\ \tau_{12} \end{bmatrix} = \begin{bmatrix} 0.5 & 0.5 & 1 \\ 0.5 & 0.5 & -1 \\ -0.5 & 0.5 & 0 \end{bmatrix} \begin{bmatrix} \sigma_x \\ 0 \\ 0 \end{bmatrix} = \begin{bmatrix} 0.5\sigma_x \\ 0.5\sigma_x \\ -0.5\sigma_x \end{bmatrix}$$

$$[\varepsilon]_{12} = [T_2][\varepsilon]_{xy}$$

for +45°:

$$\begin{bmatrix} \varepsilon_1 \\ \varepsilon_2 \\ \gamma_{12} \end{bmatrix} = \begin{bmatrix} 0.5 & 0.5 & 0.5 \\ 0.5 & 0.5 & -0.5 \\ -0.5 & 0.5 & 0 \end{bmatrix} \begin{bmatrix} \varepsilon_x \\ \varepsilon_y \\ 0 \end{bmatrix} = \begin{bmatrix} 0.5(\varepsilon_x + \varepsilon_y) \\ 0.5(\varepsilon_x + \varepsilon_y) \\ -\varepsilon_x + \varepsilon_y \end{bmatrix}$$

thus:

$$G_{12} = \frac{\tau_{12}}{\gamma_{12}} = \frac{\sigma_2}{2 \cdot (\Delta\varepsilon_x - \Delta\varepsilon_y)} \quad \tau_{12 \max} = \frac{\sigma_x \max}{2}$$

## 4 Interlaminar stresses and rate of energy release in the multilayer composite

As well as the intralaminar stresses acting in the individual layers that we have already described, interlaminar stresses can occur between the layers. The interlaminar strength ( $\tau_{ILS}$ ) of the composite during shear stress is particularly important.

In accordance with DIN EN 2563, interlaminar shear strength is determined on a short bending test specimen (length 20 mm) with a unidirectional laminate structure  $[0^\circ]$ . This structure keeps the normal stress from the bending stress low and there is failure between the layers (delamination).

Shear stress from the lateral force  $\tau_{ILS} = \frac{3 \cdot Q}{2 \cdot b \cdot h}$

So for the 3-point bending test:  $Q = \frac{F}{2}$  and thus  $\tau_{ILS} = 0.75 \cdot \frac{F}{b \cdot h}$

A further important characteristic quantity for determining the quality of the composite with regard to delamination failure, is the interlaminar rate of energy release  $G_{1C}$ , in accordance with DIN 65 563. This measures the energy that is necessary to delaminate the composite when pulling it apart, as shown in Fig. 4.1-1. The interlaminar fracture toughness is calculated from the energy consumed  $w$ , divided by the product from the crack propagation  $\Delta a$  and the width of the test specimen  $b$ :

$$G_{1C} = \frac{w}{\Delta a \cdot b} \text{ in [J/mm}^2\text{]}$$

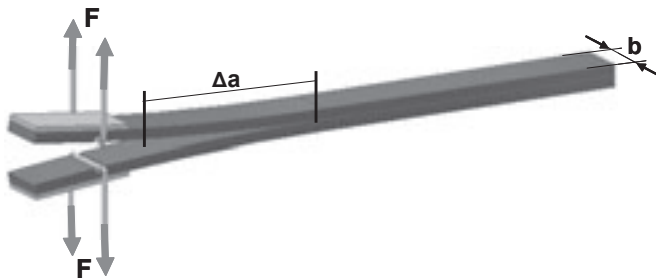


Fig. 4.1-1: Determining the interlaminar rate of energy release  $G_{1C}$

## 5 Integrating strain gages

It is a prerequisite of strain gage integration for the structure and function of the strain gage to be suitable for the special structural mechanics requirements of fiber composites, as well as the metrological requirements of strain gage measurement technology.

### 5.1 Structural mechanical aspects

#### 5.1.1 The effect of integration on the interlaminar properties of the composite

Investigations show that the strain gage attaches exceedingly well to all the usual fiber composite matrix resins:

- Hand lay-up laminate resin (L20 epoxy resin with SL hardener, made by Bakelite)
- Prepreg resin with EP matrix (hardening at 120 and 180°C)

This attachment allows the level of strain on the composite to be transferred in full to the strain gage measuring grid.

The quality of the strain gage attachment to the matrix resin was defined by means of the interlaminar shear strength ILS and the interlaminar rate of energy release  $G_{1c}$  (see Chapter 4). The investigations were based on DIN 65563 and DIN EN 2563.

The test specimens were made from unidirectional CFP prepreg material (Hexply 6376C–HTA(12K)-10-35% 300MM) and were cured in an autoclave at 180°C and 7 bar pressure.

Pre-treated polyimide foils were embedded in the symmetry plane of the test specimen and compared with reference samples without foils. The results are shown in Table 5.1.1-1.

	Rate of energy release $G_{1c}$ [J/m <sup>2</sup> ]	Shear strength ILS [MPa]
Reference samples without foil	275	120
Test specimens with foil (pre-treated)	1,030	115

Table 5.1.1-1: Results of the investigations on the attachment of polyimide foils to matrix resin 6376C-HTA

These values relate to the attachment between the strain gage carrier foil or strain gage covering foil and the fiber composite.

Investigations show that for laminates with low fracture toughness, such as hand lay-up laminates or laminates that have been produced by an injection process, no effect and sometimes higher characteristic values, were measured.

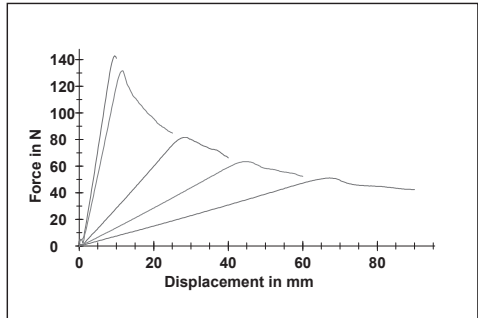
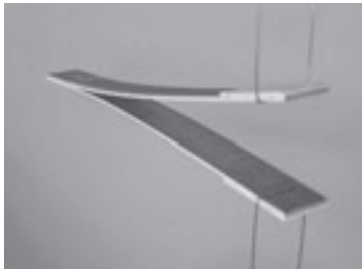


Fig. 5.1.1-1: Determining the interlaminar rate of energy release  $G_{1c}$

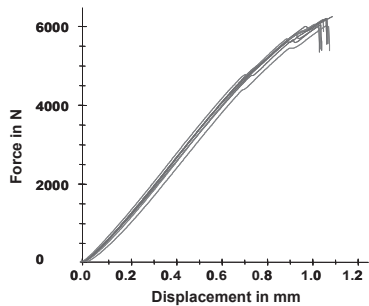


Fig. 5.1.1-2: Determining the interlaminar shear strength ILS

Thanks to the strain gage integration concept of using contact pins, disruption to the composite is reduced to a minimum, as the cabling is not embedded, but takes place outside the material. The interlaminar properties of the composite are only affected at the point of integration, which is metrologically recorded by the strain gage.

### 5.1.2 The effect of the orientation of adjacent layers on measurement accuracy

Investigations show that the measurement accuracy of the integrated strain gage in the measuring grid direction is not affected by the fiber orientation of the adjacent layers. From the metrological viewpoint, this means that in principle, the strain gage can be integrated between any of the single layers, whatever the orientation.

But ideally, the strain gage will be integrated so that its carrier foil comes to rest on the layer where the force flow is to be measured and monitored. The direction of the measuring grid will then coincide with the fiber orientation of an adjacent layer.

### 5.1.3 Depth of strain gage integration for reducing the level of strain

The permissible strain level of fiber composites and strain gages differs subject to the application and this difference is sometimes considerable. Whereas, even with a high number of load cycles, fiber composites can be stressed to over  $\pm 4,000 \mu\text{m/m}$ , the permissible strain level for strain gages is far lower.

With a small number of load cycles (up to 100 cycles), a strain gage can be loaded at over  $\pm 4,000 \mu\text{m/m}$ . But the permissible strain for endurance strength is about  $\pm 1,500 \mu\text{m/m}$  (see Fig. 5.1.3-2).

With components subjected to bending stress, integrating the strain gage can reduce its strain loading. To absorb the bending moment, the bending stress develops a tensile loaded and a compression loaded side. With fiber composites as with isotropic materials, there is a linear strain gradient over the cross-section of the test specimen.

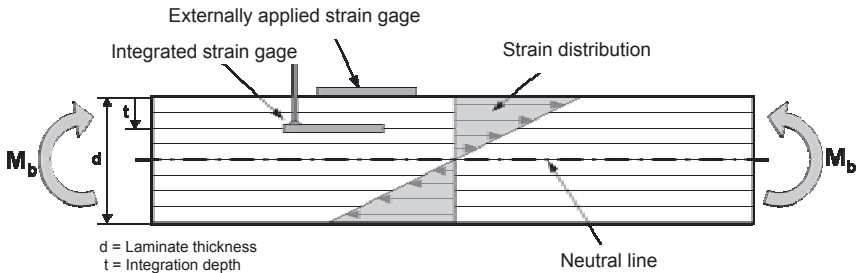


Fig. 5.1.3-1: Strain level of an integrated and externally applied strain gage on components subjected to bending stress

Thus, pure bending load produces the following correlation between the depth of integration and level of strain:

$$\frac{\mathcal{E}_{external}}{0.5 * d} = \frac{\mathcal{E}_{int}}{0.5 * (d - t)} \quad d = \text{component thickness; } t = \text{integration depth}$$

The fact that the structure can be loaded with normal stresses consisting of tensile and compressive forces, as well as the bending stress, must also be taken into account. Such normal stresses give rise to deformations, that are superimposed on the strains from the bending load. If the strain gage is arranged in the symmetry plane, the strain-dependent, measurable change in its resistance will be principally defined by the tensile and compressive forces, even for parts that are subjected to bending load.

The extent of the permissible strain level for the strain gage is based on the prescribed possible number of load cycles, subject to the resultant error fractions. Also refer to [7].

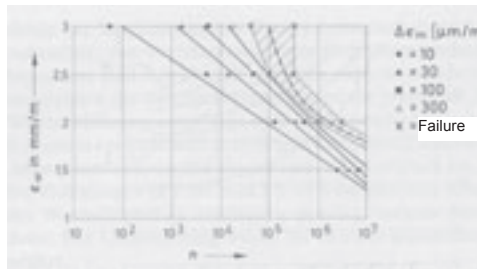


Fig. 5.1.3-2: Fatigue life of a strain gage based on constantan (from [7])

### 5.1.4 Dependency of measurement error on strain gage orientation

Below we investigate the effect on measurement accuracy of an integrated strain gage that is displaced by angle  $\varphi$  to optimize the installation position. This is of particular interest, as after the laminate curing process, the position of the integrated strain gage cannot be changed, making adjustment impossible. Should a strain gage slip out of position during the curing process, the expected measurement error can be calculated and compensated for in the result.

With a uniaxial stress state, strains  $\varepsilon_1$  and  $\varepsilon_2$  occur. Strains  $\varepsilon_x$  and  $\varepsilon_y$  result in the local strain gage system from deviation  $\varphi$  of the strain gage, in relation to the direction of principal normal stress.

Measuring grid orientation is in the x direction. It acts in these directions

1:  $E_{11}; \nu_{12}; \sigma_{max}; \varepsilon_{max}$

2:  $E_{22}; \nu_{21}; \varepsilon_q$

x:  $E_x = E_{11}(\varphi); \nu_{12}(\varphi); \sigma_x = \sigma_1(\varphi); \varepsilon_x; \varepsilon_{qy}$

y:  $E_y = E_{22}(\varphi); \nu_{21}(\varphi); \sigma_y = \sigma_1(\varphi+90^\circ)$ .

Strain  $\varepsilon_x$  is caused by stress  $\sigma_x$ .

Thus:

$$\varepsilon_x = \frac{\sigma_x}{E_x} = \frac{\sigma_1(\varphi)}{E_{11}(\varphi)}$$

With the angle-dependent stress fraction

$$\sigma_1(\varphi) = \sigma_{max} \cdot \cos^2(\varphi)$$

strain  $\varepsilon_x$  is produced in the local strain gage system

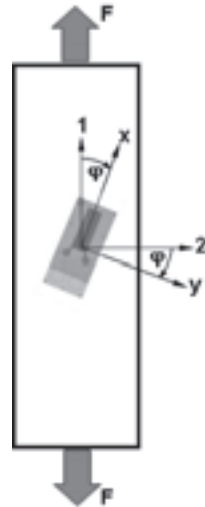


Fig. 5.1.4-1: Typical uniaxial stress state shown on a tensile test specimen



$$\varepsilon_x = \frac{\sigma_{\max}}{E_{11}(\varphi)} \cdot \cos^2(\varphi).$$

In direction x, stress  $\sigma_y$  creates transverse strain  $\varepsilon_{qy}$ , which is defined by the modulus of elasticity  $E_{22}(\varphi)$  and the Poisson's ratio  $\nu_{21}(\varphi)$ :

$$\varepsilon_{qy} = -\nu_{21}(\varphi) \cdot \frac{\sigma_y}{E_y} = -\nu_{21}(\varphi) \cdot \frac{\sigma_1(\varphi + 90^\circ)}{E_{22}(\varphi)}$$

If the angle-dependent stress fraction

$$\sigma_1(\varphi + 90^\circ) = \sigma_{\max} \cdot \cos^2(\varphi + 90^\circ)$$

is used in the above formula, the following strain is obtained

$$\varepsilon_{qy} = -\nu_{21}(\varphi) \cdot \frac{\sigma_{\max}}{E_{22}(\varphi)} \cdot \cos^2(\varphi + 90^\circ).$$

The two strains acting in the same direction can be added up, as these are strain  $\varepsilon_x$  and transverse strain  $\varepsilon_{qy}$  in direction x in the local x-y system:

$$\mathcal{E}(\varphi) = \varepsilon_x + \varepsilon_{qy}$$

This produces the following relation:

$$\mathcal{E}(\varphi) = \frac{\sigma_{\max}}{E_{11}(\varphi)} \cdot \cos^2(\varphi) - \nu_{21}(\varphi) \cdot \frac{\sigma_{\max}}{E_{22}(\varphi)} \cdot \cos^2(\varphi + 90^\circ)$$

Also applicable is the correlation (Maxwell-Betti relation) between the modulus of elasticity and the Poisson's ratios (see Section 2.5):

$$\frac{E_{11}(\varphi)}{\nu_{12}(\varphi)} = \frac{E_{22}(\varphi)}{\nu_{21}(\varphi)}$$

This results in

$$\mathcal{E}(\varphi) = \frac{\sigma_{\max}}{E_{11}(\varphi)} \cdot \cos^2(\varphi) - \nu_{12}(\varphi) \cdot \frac{\sigma_{\max}}{E_{11}(\varphi)} \cdot \cos^2(\varphi + 90^\circ)$$

the trigonometric correlation  $\cos(\varphi + 90^\circ) = \sin(\varphi)$ , produces the following for  $\mathcal{E}(\varphi)$

$$\varepsilon(\varphi) = \frac{\sigma_{\max}}{E_{11}(\varphi)} \cdot (\cos^2(\varphi) - \nu_{12}(\varphi) \cdot \sin^2(\varphi)) .$$

If addition and subtraction occur in the bracket with  $\sin^2(\varphi)$ , then you get

$$\varepsilon(\varphi) = \frac{\sigma_{\max}}{E_{11}(\varphi)} \cdot (\cos^2(\varphi) + \sin^2(\varphi) - \sin^2(\varphi) - \nu_{12}(\varphi) \sin^2(\varphi))$$

or

$$\varepsilon(\varphi) = \frac{\sigma_{\max}}{E_{11}(\varphi)} \cdot (\cos^2(\varphi) + \sin^2(\varphi) - (1 + \nu_{12}(\varphi)) \sin^2(\varphi)) .$$

To simplify the formula, use  $\cos^2(\varphi) + \sin^2(\varphi) = 1$  . This gives the definitive formula for the strain  $\varepsilon(\varphi)$  measured by the strain gage

$$\varepsilon(\varphi) = \frac{\sigma_{\max}}{E_{11}(\varphi)} \cdot (1 - (1 + \nu_{12}(\varphi)) \cdot \sin^2(\varphi))$$

The actual strain  $\varepsilon_{\max}$  in direction1 can be calculated from  $\frac{\sigma_{\max}}{E_{11}}$  .

$$\varepsilon_{\max} = \frac{\varepsilon(\varphi) \cdot E_{11}(\varphi)}{E_{11} \cdot (1 - (1 + \nu_{12}(\varphi)) \cdot \sin^2(\varphi))}$$

Which for the measurement error, gives:

$$f = \frac{\varepsilon(\varphi) - \varepsilon_{\max}}{\varepsilon_{\max}}$$

Because of the directional dependency of the material response ( $E_{11}$ ,  $E_{22}$ ,  $G_{12}$ ,  $\nu_{12}$ ) of fiber composites, it is frequently necessary when calculating, especially when summarizing the stiffnesses in multiaxial laminates, to transform the stresses and distortions from the 1-2 principal axis system of the material to a global x-y coordinate system, and vice versa.

To make these established findings clearer, there now follow some examples of typical fiber composites made from GFP and CFP. In these examples, the test specimens are made of unidirectional layers, the orientation of which is always in the  $0^\circ$  direction  $[0^\circ, 0^\circ, 0^\circ, 0^\circ]_{\text{sym}}$ . This gives an extremely strong directional dependency for the moduli of elasticity and the Poisson's ratios. A quasi-isotropic laminate structure  $[+45^\circ, 0^\circ, -45^\circ, 90^\circ]_{\text{sym}}$  made from GFP and CFP was chosen for reference. To establish evidence about the relative measurement error, a maximum practical strain level of  $\varepsilon_x = 0.5\%$  is assumed and the maximum stress associated with this of  $\sigma_x$  is calculated. The diagrams below show the material constants of the examples just listed in polar coordinates.

The top left graphic in Fig. 5.1.4-2 shows the strong directional dependency of the modulus of elasticity of the anisotropic laminate with the structure  $[0^\circ]_4$  sym. The maximum modulus of elasticity is only available exactly along the fiber orientation, that is in the  $0^\circ$  direction. Even with slight deviations, the modulus of elasticity is noticeably lower – a deviation of  $10^\circ$  results in a reduction in the modulus of elasticity of 50%. Compared with this, it is clear from Fig. 5.1.4-4 that the material properties for quasi-isotropic laminates are the same in all directions.

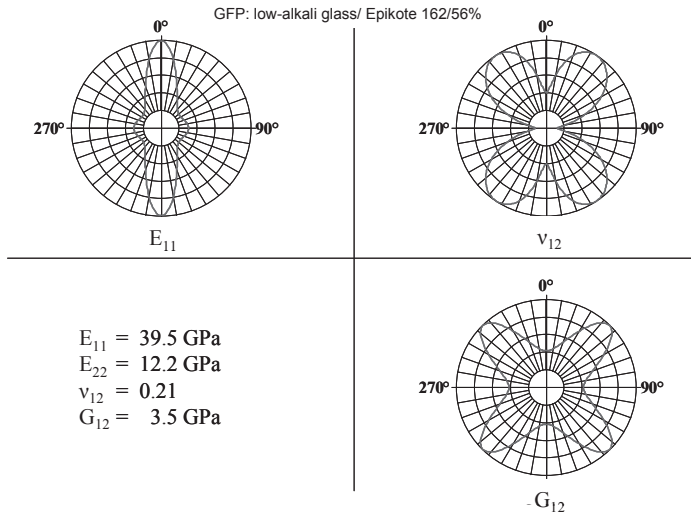


Fig. 5.1.4-2: Material characteristics for the anisotropic laminate structure made from GFP  $[0^\circ]_4$ , sym

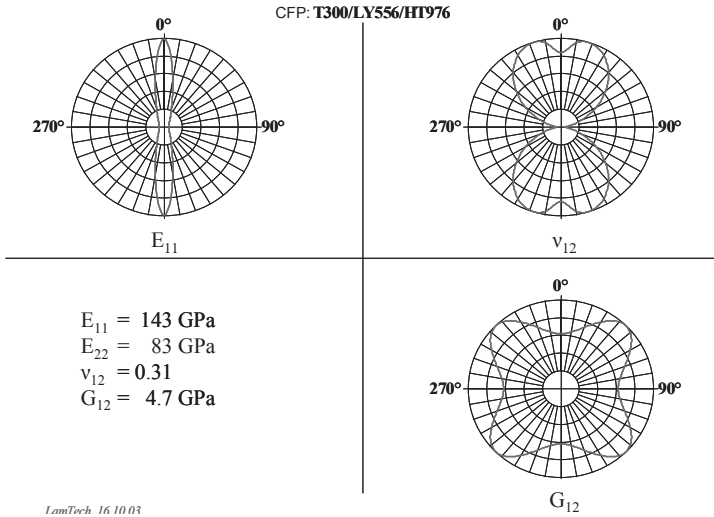
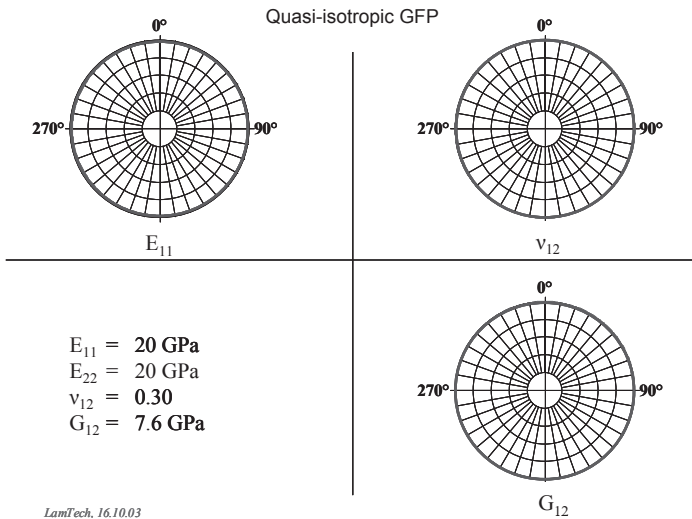


Fig. 5.1.4-3: Material characteristics for the anisotropic laminate structure made from CFP  $[0^{\circ}]_4, \text{sym}$

Fig. 5.1.4-4: Material characteristics for the quasi-isotropic laminate structure made from GFP  $[+45, -45, 90]_{\text{sym}}$



$0, -45, 90]_{\text{sym}}$

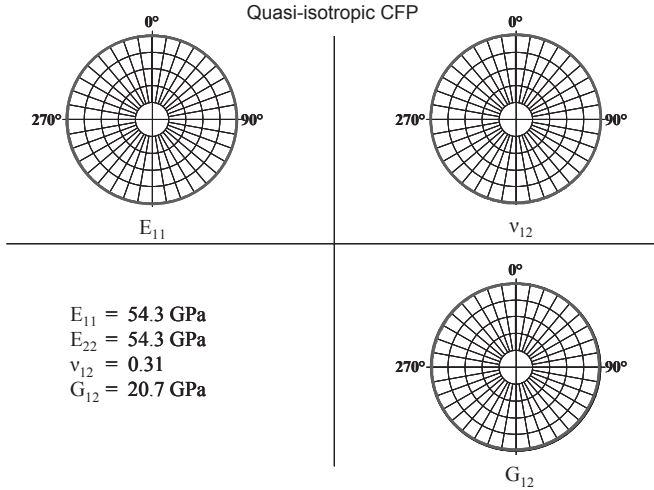


Fig. 5.1.4-5: Material characteristics for the quasi-isotropic laminate structure made from CFP [+45, 0, -45, 90]<sub>sym</sub>

In the following chart (see Fig. 5.1.4-6), the relative measurement error ( $f = \frac{\varepsilon(\varphi) - \varepsilon_{\max}}{\varepsilon_{\max}}$ ) is plotted over the angular variation of the strain gage to the direction of principal stress. The range of 0° to 5° angular variation shown here is of practical interest.

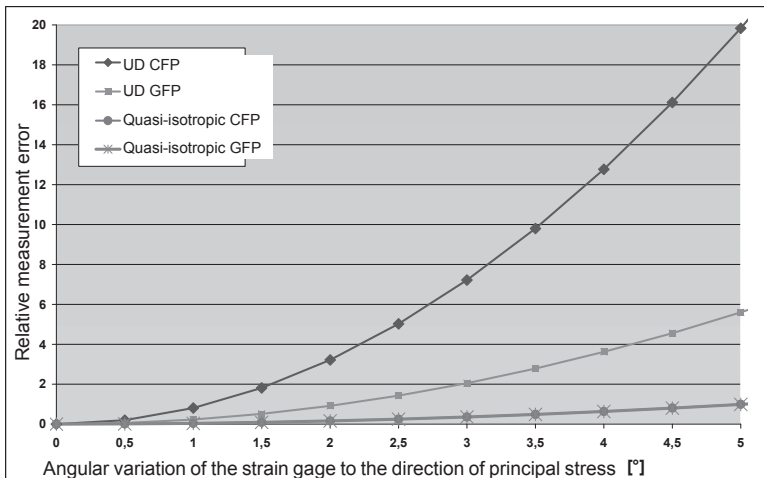


Fig. 5.1.4-6: Relative measurement error for different materials and laminate structures

This chart shows particularly clearly how great an effect the material and its orientation have on the measurement error. The greatest error occurs with CFP laminates that are only made up of UD layers. With GFP laminates, the error with the same layer structure is far less. The progression of the characteristic curves of the errors of both the quasi-isotropic laminates are virtually identical. This is made clear by simplifying the previously derived formula. The formula for quasi-isotropic materials ( $E_{11} = E_{11}(\varphi)$ ;  $\nu_{12} = \nu_{12}(\varphi)$ ) goes:

$$\varepsilon_1(\varphi) = \varepsilon_{\max} \left[ 1 - (1 + \nu_{12}) \cdot \sin^2(\varphi) \right]$$

The transverse contraction  $\nu_{12}$  is decisive for relative error in quasi-isotropic materials. This means that with the same strain gage deviation from the direction of principal stress, the relative error for quasi-isotropic laminates with the same Poisson's ratio is identical. In this situation, the transverse contractions for both the quasi-isotropic laminates is 0.3.

The examples have demonstrated that relative measurement error is dependent on two essential factors, firstly on the choice of material and secondly on its laminate structure.

This is reflected in the quotients  $\frac{E_{11}}{E_{22}}$  and  $\frac{\nu_{12}}{\nu_{21}}$ . In summary, this means: the greater

$\frac{E_{11}}{E_{22}}$  or  $\frac{\nu_{12}}{\nu_{21}}$  (UD CFP, for example), the greater the relative measurement error when the strain gage deviates from the direction of principal stress. These investigations all relate to the uniaxial stress state.

### 5.1.5 The effect of heat generation for integrated strain gages

Fiber composites have very low thermal conductivity. To minimize the rise in temperature of the integrated strain gage, the strain gages that are used for integration have an electrical resistance of 350 ohms. Furthermore, the excitation voltage should not exceed 2.5 V.

To achieve stationary conditions, it is advisable, with exacting accuracy requirements, to activate the measuring point for a similar length of time to the downstream electronics (about 15 to 30 minutes), before actually taking the measurement.

### 5.1.6 Temperature compensation for fiber composites

Fiber composites with directional continuous fibers can have directionally dependent thermal expansion coefficients (see Sections 2.4, 3.2.4 and 3.7). This anisotropy must be taken into account during temperature compensation.

The compensating strain gage must therefore show the same orientation on the compensating element as that of the strain gage used for measurement on the measurement object.

Only laminates with a quasi-isotropic laminate structure have a thermal expansion response that is not directionally dependent. In this situation, it is not necessary for the strain gages that are used for compensation and for measurement to have the same orientation.

### 5.1.7 Effect of transverse sensitivity

In principle, strain gages are constructed so that even when stress is superimposed, the only strains to be measured are those in the measuring grid direction  $\varepsilon_l$ . A strain across the measuring grid direction  $\varepsilon_q$  influences the measurement signal to a small proportion. This proportion is described by the transverse sensitivity  $q$  of the strain gage and is 0 to 0.1%.

For traditional reasons, strain gages are calibrated for materials with a Poisson's ratio  $\nu_0$  of 0.285. If measurements are taken on materials with this Poisson's ratio under a uniaxial loading, there will be no measurement error, even with strain gages with transverse sensitivity.

With fiber composites, because of the anisotropic material properties, there can be very different Poisson's ratios in the 0.01 to over 0.7 range. Whereas laminates with quasi-isotropic laminate structures have Poisson's ratios in the range 0.25 to 0.35, the Poisson's ratios for laminates with the  $\pm 45^\circ$  structure can assume values of 0.7 and laminates with the  $90^\circ$  structure, values of 0.01.

The measurement error  $f$  can be calculated in accordance with the following formula [7]:

$$f = \frac{q}{1 - q \cdot \nu_0} \cdot \left( \frac{\varepsilon_q}{\varepsilon_l} + \nu_0 \right)$$

This can determine the actual stress. The following is then applicable:

$$\varepsilon = \frac{\varepsilon_{meas}}{1 + f}$$

As is shown in the following examples, the effect can usually be ignored.

**Example 1:**

Using strain gages to determine the intralaminar shear modulus  $G_{12}$  on the  $\pm 45^\circ$  tensile test specimen in accordance with EN ISO 6031.

Laminate structure [+45,-45,-45,+45]

Transverse sensitivity of the strain gages  $q = 0.1\% = 0.001$

Poisson's ratio of the laminate  $\nu_{12} = 0.7$

Poisson's ratio of the calibration beam  $\nu_0 = 0.285$

Measured strain in the force direction:  $\varepsilon_1 = \varepsilon_{\text{meas}} = 2500 \mu\text{m/m}$

Transverse strain:  $\varepsilon_q = -1750 \mu\text{m/m}$

1.1 Strain gage in the force direction

$$f = \frac{0.001}{1 - 0.001 \cdot 0.285} \cdot \left( \frac{-1750}{2500} + 0.285 \right) = -0.042\%$$

$$\varepsilon = \frac{2500 \frac{\mu\text{m}}{\text{m}}}{1 - 0.000415} = \underline{\underline{2501 \frac{\mu\text{m}}{\text{m}}}}$$

1.2 Strain gage across the force direction

$$f = \frac{0.001}{1 - 0.001 \cdot 0.285} \cdot \left( \frac{2500}{-1750} + 0.285 \right) = -0.11\%$$

$$\varepsilon = \frac{-1750}{1 - 0.00114} = \underline{\underline{-1752 \frac{\mu\text{m}}{\text{m}}}}$$

In the longitudinal direction ( $\varepsilon_1$ ), there is a measurement error of 0.042% for the strain gage. For the strain gage turned by  $90^\circ$  to determine the transverse strain, there is a measuring error of 0.11%. In practice, the error when determining the shear modulus with the formula according to Section 2.2 is negligible.



## Example 2:

Using strain gages to determine the modulus of elasticity  $E_{11}$  and the transverse strain  $\nu_{12}$  on the  $0^\circ$  tensile test specimen in accordance with EN ISO 527-4.

Laminate structure	[0,0,0,0]
Transverse sensitivity of the strain gages	$q = 0.1\% = 0.001$
Poisson's ratio of the laminate	$\nu_{12} = 0.3$
Poisson's ratio of the calibration beam	$\nu_0 = 0.285$
Measured strain in the force direction:	$\varepsilon_l = \varepsilon_{\text{meas}} = 2500 \mu\text{m/m}$
Transverse strain:	$\varepsilon_q = -750 \mu\text{m/m}$

### 2.1 Strain gage in the force direction

$$f = \frac{0.001}{1 - 0.001 \cdot 0.285} \cdot \left( \frac{-750}{2500} + 0.285 \right) = -0.0015\%$$

$$\varepsilon = \frac{-750 \frac{\mu\text{m}}{\text{m}}}{1 - 0.000015} = \underline{\underline{-750.01 \frac{\mu\text{m}}{\text{m}}}}$$

### 2.2 Strain gage across the force direction

$$f = \frac{0.001}{1 - 0.001 \cdot 0.285} \cdot \left( \frac{2500}{-750} + 0.285 \right) = -0.3\%$$

$$\varepsilon = \frac{-750}{1 - 0.003} = \underline{\underline{-752 \frac{\mu\text{m}}{\text{m}}}}$$

In this situation as well, the measurement error is clearly less than the usual material dispersion for fiber composites caused by the manufacturing tolerances.

### 5.1.8 Effect of strain gage sensitivity perpendicular to the measuring grid plane

Strain gages that are applied to the surface are generally deformed by the longitudinal strain  $\epsilon_x$  and the transverse strain  $\epsilon_y$  that occur in the measuring grid plane.

In contrast, integrated strain gages are also stressed perpendicularly to the measuring grid plane [10]. The level of stress depends on the modulus of elasticity of the material in the thickness direction  $E_z$  and the corresponding Poisson's ratios  $\nu_{zx}$  and  $\nu_{zy}$ .

The modulus of elasticity of fiber composites in thickness direction  $E_z$  is low, compared to the moduli of elasticity in the laminate plane. With unidirectionally reinforced materials with directional continuous fibers,  $E_z$  is usually equated with the modulus of the single layer across the fiber direction  $E_{22}$  (6,000 to 12,000 MPa) (also see [11]). Depending on the structure of the laminate, Poisson's ratios  $\nu_{zx}$  and  $\nu_{zy}$  will fall in the range 0.25 to 0.35. For deformations in the thickness direction ( $\sigma_z = 0$ ) applies:

$$\epsilon_z = -\frac{\nu_{zx}}{\epsilon_x} \cdot \sigma_x - \frac{\nu_{zy}}{\epsilon_y} \cdot \sigma_y$$

In principle, this stress causes a change of resistance in the strain gage, which is superimposed on the strain gage signal as an error. Depending on the type of loading (tensile or compressive), the change in resistance can be positive or negative. The level of measurement error depends on the sensitivity of the strain gage perpendicular to the measuring grid plane, which is about  $0.55 \pm 0.2 \mu\text{m}/(\text{mMPa})$  [7,10]. In the usual strain range, measurement error is less than 0.2% and can therefore be ignored for many practical applications.

As described in Chapter 3, as part of the development of integrated strain gages with contact pins, comparative investigations were carried out with strain gages attached to the surface. Different laminate structures ( $0^\circ$ ,  $\pm 45^\circ$ , quasi-isotropic) with vastly different material characteristics were tested. In all the tests, there were measurement tolerances of up to 3% between the integrated strain gages and those attached to the surface.

## 5.2 Description of the strain gage

HBM has developed strain gages (see example in Fig. 5.2-1) suitable for integration in fiber composites that satisfy the special structural mechanical and production engineering requirements of the material as well as the metrological requirements of strain gage measurement technology.

The most obvious feature of this strain gage is the two vertically attached contact pins, for contacting the strain gage embedded in the material. The gold-plated pins are given special insulation so that they can be integrated into electrically conductive carbon fibers.

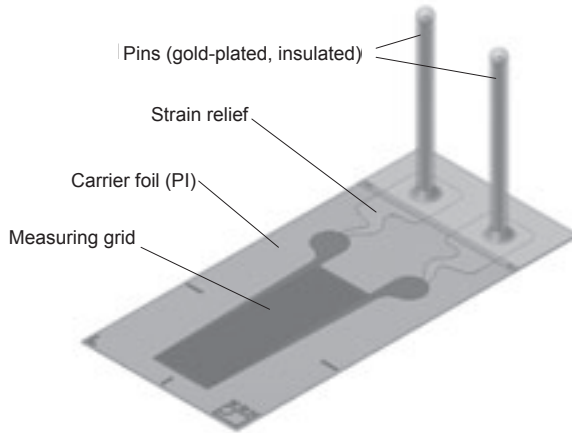


Fig. 5.2-1: Strain gage with contact pins

The special layout of the strain gage is designed so that the areas where the fibers are displaced by the pins are not part of the measuring grid area. This allows a homogeneous distribution of the material above and below the measuring grid.

Furthermore, special strain relief of the solder terminals prevents the forces working on the pin from being transferred to the measuring grid.

In principle, the strain gage is suitable for all current processing methods and materials (prepreg or dry fiber) and is resistant to a temperature of 200°C.

### 5.2.1 Structure and attachment of the strain gage

In contrast to the usual strain gage application on the surface of a component, where a special adhesive is used to glue the relevant side of the strain gage, with integration, the strain gage is attached to the material on both sides by the matrix resin in the production process.

The best possible adhesion is required between the strain gage and the matrix resin (usually EP), so that if possible, the strains are transferred to the measuring grid loss-free. This is ensured by a special pre-treatment of the covering and carrier foils of the strain gage.

## 5.2.2 Function of strain gage contact pins

In its embedded state, the strain gage is no longer accessible from outside, making it impossible for the measuring leads to contact the solder terminals. So the strain gage design had to make it possible for contact to be made afterwards.

Embedding a fully wired strain gage, that is, a strain gage with the relevant measuring leads is not advisable for a number of reasons:

### 1. The effects on the measured values and the disruption to the composite

Embedding the measuring leads causes them to stick to the laminate and the structural deformations are transferred to the measuring leads. The strain on the measuring leads also causes a change in resistance, which has an effect on the measured value. In principle, to prevent this effect, it is possible to use Teflon insulated wires that do not stick to the resin. But the disruption to the composite caused by the wires is rated as critical, as in principle, a "defect" is being inserted.

### 2. Effect on the structural mechanical properties of the laminate

Several strain gages are often needed in the stress analysis of a structure, to establish evidence of the loading situation. It is useful to contact the strain gages in a three-wire circuit, to compensate for measurement errors caused by a change in the thermal resistance of the leads [12]. Even with a small number of 3 strain gages for measuring in the 0°, 90° and 45° directions, the number of measuring leads required quickly accumulates (9 are needed for a 3-wire circuit). So from the structural mechanical viewpoint, even with a small number of strain gages, it is already unacceptable to integrate the measuring leads, as this would cause considerable disruption to the laminate.

The wires should at least be installed in a defined direction within the structure, such as with the same orientation as the fibers, to keep the effect as much in the same direction as possible. But the production engineering costs for this would be prohibitive.

So for the reasons stated above, the strain gage for integration is designed so that the wiring can be added after it has been integrated in the laminate. This is achieved by providing two contact pins, pins for short, that are attached perpendicularly to the solder terminals of the strain gage (see Fig. 5.2-1). The pins allow strain gage integration and strain gage contacting to be separate operations. There are a number of crucial advantages to this vertical pin arrangement:

- a) The contact elements take the shortest route out of the laminate, thus reducing to a minimum the effects of possible disruption to the laminate. The load-bearing fibers are not damaged by the pins.
- b) The strain gage is fixed by the pins, as the pins poke through the individual fiber layers and are held in place by the surrounding fibers.

- c) Handling during production is far simpler, as there are no wires to be run through the structure. The pins poke through the individual layers and go directly through to the surface.

When strain gages are integrated into electrically conductive CFP materials, the pins are coated with a special insulation.

Depending on the requirement, the user can decide whether the pins should be contacted inside the structure or on the outside. Thus, for example, with sandwich structures, the measuring leads or customized electronics can be introduced into the foam core.

### 5.2.3 Technical properties of the strain gage

Technical properties of a strain gage, using strain gage type LI66-10/350 as an example:

**Strain gage:**

Dimensions (L x W):	22 x 10 mm
Carrier / covering foil	Polyimide
Measuring grid material:	Constantan
Size of measuring grid:	10 mm
Resistance:	350 $\Omega$
Temperature compensation:	$\alpha = 0.5 \cdot 10^{-6} [1/K]$

**Pins:**

Material:	Brass
Finish:	Gold over nickel
Pin length:	15 mm
Pin diameter:	0.6 mm
Maximum processing temperature:	200°C.

## 5.3 Strain gage integration

The integration technique is described for bonded fabrics with dry fibers. Prepreg processing is only slightly different. The differences are pointed out where relevant.

### 5.3.1 Strain gage positioning

The exact position and alignment of the strain gage is crucial for the later assessment of the stress state. With installation on the surface, the strain gage is aligned on the finished component. This is usually done by making marks on the surface in the form of scribed lines and then aligning the strain gage to these during the installation process.

With integration, the strain gage is aligned and installed on the bonded fabric during production. As it is not possible to use a scribe or a pen to make marks on this surface, it is necessary to fall back on alternatives to marking. For small structures ( $<1 \text{ m}^2$ ), conventional measuring tools such as an angle gage and a ruler are sufficient for checking the position and the alignment. With complex structures, or when integrating several strain gages, it is also possible to prepare an installation template, that can be fixed to or inserted in the molding tool while the strain gage is being positioned (see Fig. 5.3.1-1a).

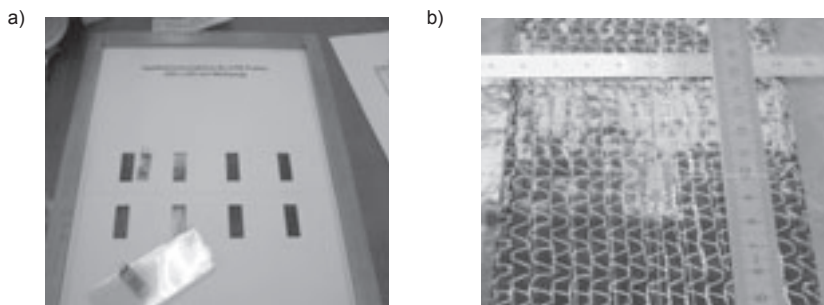


Fig. 5.3.1-1: Strain gage positioning and alignment

- a) installation template inserted in the molding tool
- b) threads stretched along the structure – a ruler is used for precise alignment

With large components ( $>1 \text{ m}^2$ ), one marking option is to use several threads stretched along the structure. This produces orientation lines, which aid exact alignment with a ruler and an angle gage (see Fig. 5.3.1-1b). Another option is to use laser projectors, which possibly are already being used in the production process. These can display precise images onto the fiber mats, thus marking the exact position.

### 5.3.2 Strain gage fixing

During the production process, when processing the dry fiber material, there is a risk that this handling may cause the strain gage to slip. To prevent this, the strain gage must be held in place some other way, until it is fixed by the covering foam (see Section 5.3.4). When using an adhesive to fix the strain gage to dry fibers, you must take into account that in this area, neither the fibers nor the strain gage can subsequently be impregnated with the matrix resin. So there are two possible alternative fixing options:

#### a) Using a binder powder

A common method of fixing the fiber mats together when processing dry fiber material is to use so-called binder powder. This binder powder consists of a thermoplastic material, which for fixing, is spread between the fiber mats and melted at about 80°C. Once the powder has cooled, the mats are “fused” together, thus producing a sort of preform.

This method can also be used to fix the strain gages. But as the use of this binder is restricted to certain production techniques or it may not always be desirable to introduce the binder, the powder can equally well be spread using a template to restrict it to the local area around the installation point (see Fig. 5.3.2-1a)). The binder powder should be spread in such a way as to give an even distribution and to use as little powder as possible. It is essential to prevent an enclosed powder coating. Using a sieve is a good way to control the spread and amount of powder used.

Once the binder has been spread, the strain gage is placed on the fiber material and aligned. To heat the binder, you need a heatable tool (such as the special electric iron made by Graupner), which melts the binder at 80°C. During this fusion, the strain gage should also be covered by a thin sheet of Teflon foil. This prevents the tool coming into direct contact with the binder and stops it getting dirty. Light pressure for about 20 seconds is enough to melt the binder and fuse the strain gage to the fiber material.

A considerable advantage of using binder powder is that melting takes place while the laminate is curing. This makes it possible to impregnate with resin the strain gage foil and the fibers that were in contact with the binder.

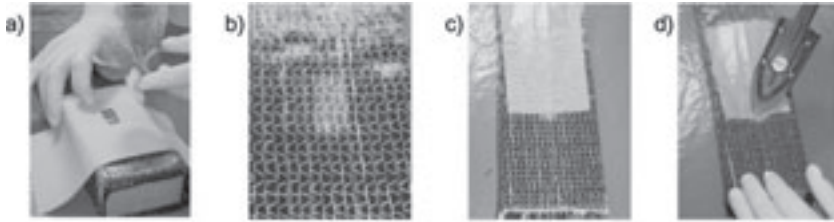


Fig. 5.3.2-1: Fixing the strain gage with binder powder

- a. using a covering template and a sieve to apply the binder to the local area
- b. light binder coating in the installation area
- c. Teflon foil placed on the strain gage
- d. using a special electric iron to fuse the strain gage

#### b) Using special tack sprays

Another way to fix the strain gage is to use special spray adhesives (tack sprays), which are used to fix fiber mats and peel plies. These adhesives generate a “tack” (tackiness) such as that which is already available in prepreg material. A light mist spray on the application side of the strain gage is sufficient for fixing. Once it has been sprayed with tack spray, the strain gage is placed on the fiber mat as described in a).

With prepreg materials, it is not necessary to fix the strain gage as described in a) and b), as adequate fixing for the strain gage is already provided by the tack of the material. So the strain gage can be applied directly to the material.

In principle, you should avoid making frequent adjustments to the position of the strain gage during the installation process by repeatedly pulling it off and reattaching it, so that you do not impair the measurement properties of the strain gage.

### 5.3.3 Laminating and applying more layers

The construction of the fibers and the depth of integration determine how production is to continue for the structure. There are basically two preferred options:

#### 1. The strain gage is applied to the fibers with the pins facing upward.

This means that when further layers are put in place – fiber mats, peel plies, membranes, etc. – the pins poke through each of the layers as they are added. Care should be taken, in accordance with the type and thickness of the layers, to ensure that pins do not become damaged. With thin single layers (< 1mm) made from a unidirectional dry fiber material, there is no problem pushing the pins through. It is more difficult with a prepreg material and multi-axial dry fiber layers with layer thicknesses greater than 0.5 mm. Here you must enlist the aid of a suitable tool to help the pins go through, such as first pushing through the layer with a needle.



The fiber mats should be put in place perpendicularly to the pins, as otherwise fibers may build up, or become depleted between the pins. A buildup of material between the pins will push the pins apart and conversely, a lack of material will push the pins together (see Fig. 5.3.3-1). This effect will be enhanced with every layer that is added and can ultimately damage the pins and the strain gage. So this method of installation is particularly suitable for low depths of installation, where only a small number of fiber layers are put in place.

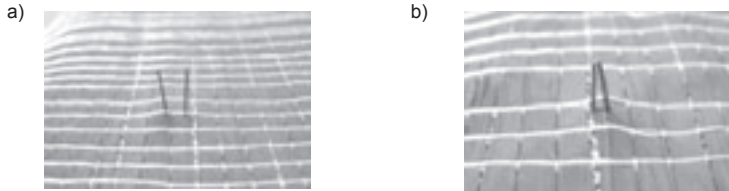


Fig. 5.3.3-1: Incorrect integration caused by the irregular distribution of the material between the pins

- a) the excess material between the pins has pushed the pins apart
- b) the lack of material between the pins has pushed the pins together

## 2. The strain gage is applied with the pins facing downward

With this production variant, the strain gage is applied so that pins poke into the material that has already been put in place (see Fig. 5.3.3-2). But this presupposes that the fiber material has been placed on a substrate that the pins can penetrate. In all cases, a needle or appropriate tool must be used to prepare for the passage of the pins.

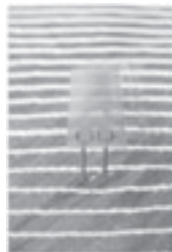


Fig. 5.3.3-2: Applying the strain gage the other way round

Once the strain gage has been applied, the additional fiber layers can be put in place. This is the preferred production method for deep integration, as subsequent fiber layers do not have to be placed over the pins individually.

### 5.3.4 Shortening and covering the pins

Before the pins are covered, they are shortened to 2 mm, as this length is sufficient for later contacting (see Fig. 5.3.4-1). The pins should only be shortened once the peel ply is in place, as the tip is rounded off to prevent the filaments catching when they push through the fiber mats. Once the pins have been shortened, the surface at the end of the pins is rough, with sharp edges and any filament-type fabric would catch on this as the pins were poked through.

A tool working on the scissor principle is not suitable for shortening the pins, as the cutting-action could bend the pins. Fine diagonal cutters, such as those used in electronics, are better suited to the job.



Fig. 5.3.4-1: Shortening pins with a diagonal cutter

Once they have been shortened, the pins should be covered. A special silicone foam that has several functions, is provided for this purpose:

3. Protecting the membrane or vacuum bag film from being damaged by the pins during production processes involving single-shell molding tool concepts.

4. Fixing the strain gage

The penetration of the pins into the silicone foam fixes the pins and thus the entire strain gage in position. This is very important, as the low viscosity of the resin means that the fixing while curing mentioned in Section 5.3.2 is no longer adequate.

5. Stopping the pins resinifying

The soft covering foam is compressed by the vacuum and pushes against the pins. This prevents the resin advancing up the pins. If a hard foam material is used, the pins are stuck to the foam by the advancing resin and will be pulled off during removal from the mold.

The size of the structure will determine whether the entire laminate is covered, or just the area where the pins are protruding. Local coverage is usually required for large

structures, with the pins being covered in such a way that the foam is thickest in the center, gradually falling away on all sides. This can be done in two ways:

From a 12 mm thick sheet of silicone foam, cut a piece approx. 60 x 60 mm in size and machine it to make a pyramid-shaped body like the one shown in Fig 5.3.4-2a).

Cut 5 – 6 different-sized square pieces (e.g. 50 x 50 mm, 40 x 40 mm, etc.), from 0.5 mm thick silicone film and stack them one on top of the other so that you again get a pyramid-shaped body (see Fig. 5.3.4-2b)).

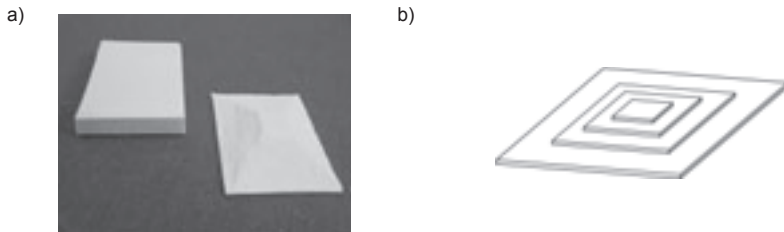


Fig. 5.3.4-2: Pin covering design variants

a) covering shaped from a silicone sheet

b) covering made from silicone layers stacked one on top of the other

A smooth transition from the pin covering to the laminate is the only way to ensure that the pin covering does not leave any impressions on the laminate.

### 5.3.5 Hints on removal from the mold

While it is not difficult to remove the vacuum bag film and the absorbent matting, as the pins are protected by the covering foam, special care must be taken when removing the peel ply. You must be particular cautious when removing the peel ply from the pin area, as if the fabric is loosened with a jerk, the pins could break off.

Tip: Deliberately make cuts in the peel ply around the pin area (see Fig. 5.3.5-1) to relieve the pressure on the pins when the fabric is removed.



Fig. 5.3.5-1: Cutting into the peel ply in the pin area

## 5.4 Connecting the measuring leads

### 5.4.1 Removing the insulation

Before the pins can be contacted, the insulation has to be removed. Under no circumstances should this be done with a soldering iron, as the high temperatures necessary for this (the insulation is resistant to heat of about 300°C) and the thermal conductivity of the pins pose the risk that all the insulation will burn off (risk of short-circuits in CFP laminates!). If exposed to high temperatures for long, the matrix resin may also suffer local burns. There is also the risk to a cold solder joint in the laminate, as at temperatures > 310°C, the solder connection between the pin and the solder terminal could melt.

It is advisable to remove the insulation by mechanically shaving it off with a scalpel or a cable stripper. As shown in Fig. 5.4.1-1, about 0.5 - 1 mm of insulation should be left above the surface of the laminate.

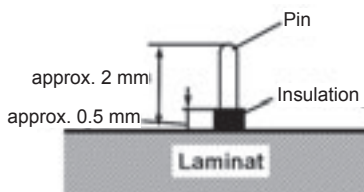


Fig. 5.4.1-1: Pin insulation

## 5.4.2 Contacting the pins

The best method of electrical connection between the pin and the measuring lead is soldering. Different applications require a different contact arrangement and the distinction must be made between statically and dynamically stressed components.

With static stress, the measuring leads can be soldered directly to the pin. To obtain a good solder connection, the measuring leads are soldered perpendicular to the pin (see Fig. 5.4.2-1). To protect the pins and stop them being damaged by pulling on the measuring leads, the measuring leads should be fixed to the component. HBM X60 superglue or a hot-melt-type adhesive, for example, are suitable for this.

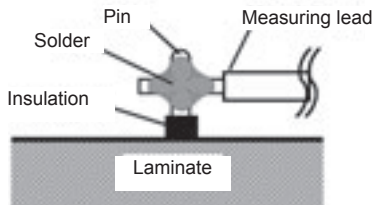


Fig. 5.4.2-1: Soldering the measuring leads to the pins

With dynamic stress, it is advisable not to solder the measuring leads directly to the pins, as the movement of the measuring leads would put them under load. Connecting an intermediate solder terminal would relieve the load on the pins and make it easier to execute a perfect solder joint. The solder terminal can be attached with a superglue such as Z70, or by double-sided adhesive tape. For dynamically loaded components with extreme strain on the edge fibers ( $> 0.1\%$ ), it is preferable to attach the solder terminal with double-sided adhesive tape, as the "soft" adhesive tape cannot transfer the strains to the solder joints.

The connection between the pin and the solder terminal must also be designed to be flexible. To achieve this, run a single wire from the pin to make an inverted arch to the solder terminal (see Fig. 5.4.2-2). With dynamically stressed components with a high number of load cycles, the measuring leads must also be run in an inverted arch to the solder terminals and the cable must be fixed by firmly attaching it to the component.

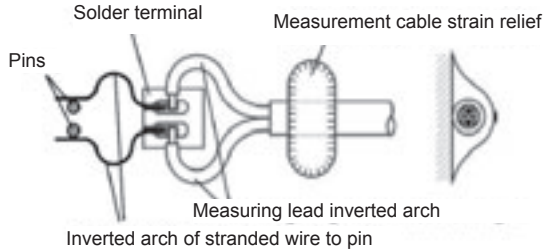


Fig. 5.4.2-2: Contacting the pins for dynamically stressed components

## 6 Measuring point protection

The steps taken to protect the measuring point are determined by the type of mechanical and chemical influences and by the side on which the pins exit the structure.

If the pins appear outside the structure on the surface, it is advisable after soldering on the measuring leads (see Section 5.4) to provide relevant protection for the solder connection and the pin exit point against the prevailing ambient conditions. Detailed descriptions of measuring point protection can be found in the separate publication "Practical hints for the installation of strain gages" (Chapter 5, [16]).

Should the pins run inside the structure, you must clarify whether additional pin protection is necessary in each individual case.

## 7 Bibliography

- [1] Robert M. Jones, Mechanics of Composite Materials, Hemisphere Publishing Corporation, New York
- [2] Manfred Flemming, Siegfried Roth, Faserverbundbauweisen – Eigenschaften, Springer-Verlag 2003, ISBN 3-540-00636-2
- [3] Gottfried W. Ehrenstein, Faserverbund-Kunststoffe, Carl Hanser Verlag, München, 2006, ISBN 3-446-22716-4
- [4] Alexander Horoschenkoff, Skripte zur Vorlesung „Kunststofftechnik“
- [5] DIN EN 2563
- [6] DIN 65563
- [7] Karl Hoffmann, Einführung in die Technik des Messens mit Dehnungsmessstreifen, Hottinger Baldwin Messtechnik GmbH, 1987
- [8] Stefan Keil, Beanspruchungsermittlung mit Dehnungsmessstreifen, Cuneus, 1995, ISBN 3-9804188-0-4
- [9] Thomas Kleckers, Dirk Eberlein: Bestimmung des einachsigen Spannungszustandes, Vortrag anlässlich „HBM on Tour“, 2002
- [10] Augusto Ajovalasit: "Embedded Strain Gauges: Effect of the Stress Normal to the Grid" Dipartimento di Meccanica, Università di Palermo, Strain (2005) 41, 95-103
- [11] Gerhard Scharr: „Experimentelle Bestimmung des kompletten Stoffgesetzes von anisotropen faserverstärkten Kunststoffen“ Messtechnische Briefe (1985), 21, Heft 1
- [12] Sebastian Klein, Entwicklung eines Konzeptes zur Strukturintegration von Dehnungsmessstreifen in Faserverbundwerkstoffen, Diplomarbeit August 2003
- [13] Carsten Hecker, Numerische und experimentelle Untersuchung des Spannungszustandes an Kontaktelementen bei strukturintegrierten DMS, Diplomarbeit Januar 2004
- [14] Thomas Kabilka, Entwicklung und Untersuchung von Konzepten zur Integration von Dehnungsmessstreifen in Faserverbundwerkstoffe, Diplomarbeit März 2004
- [15] Hotline 1/2001, Hottinger Baldwin Messtechnik GmbH
- [16] Karl Hoffmann, Hinweise zum Applizieren von Dehnungsmessstreifen, Sonderdruck VD 84005

Modifications reserved.

All details describe our products in general form only.  
They are not to be understood as express warranty  
and do not constitute any liability whatsoever.

Hottinger Baldwin Messtechnik GmbH

Postfach 100151 D-64201 Darmstadt  
Im Tiefen See 45, D-64293 Darmstadt, Germany  
el.: +49 6151 803 0 · Fax: +49 6151 803 9100  
E-mail: [info@hbm.com](mailto:info@hbm.com) · [www.hbm.com](http://www.hbm.com)



Measurement with confidence